Chapter 3

Analytical solutions and thermodynamics of binary BCC and FCC phases for exclusive second neighbour pair interactions

3.1 Introduction

The equilibrium state of a phase under the framework of CE–CVM can be obtained by minimization of the Helmholtz energy, expressed in terms of CFs which represent the configurational state of the system and CECs, apart from temperature and composition. This involves solving nonlinear equilibrium equations using numerical techniques such as Natural Iteration Method (NIM) (Anoune and Aouachria, 2011; Kikuchi, 1974; Kiyokane and Mohri, 2011; Pretti, 2005; Xingjun *et al.*, 1995) and Newton - Raphson method (Harvey *et al.*, 2013; Lele and Sarma, 2009; Yuille, 2002).

In the special case of pair approximation of quasi-chemical theory for a binary alloy, which is equivalent to the first order approximation of CE–CVM, Guggenheim (1935; 1952) obtained an analytical solution for the pair CF. For the close packed net in 2D, analytical solutions of CFs could be found for exclusive pair interactions in the triangle approximation, only at the equiatomic composition (Gorrey *et al.*, 2015; Kikuchi and Brush, 1967). Such results are not available for other types of basic clusters such as tetrahedron cluster in 3D. In this Chapter, analytical solutions for the CFs are obtained using exclusive second neighbour pair interactions for binary $A2\,\&\,B32$ phases and $A1\,\&\,L1_1$ phases respectively under T and TO approximations of CVM.

3.2 Analytical solutions for CFs in $A2$ phase

The formulation of CE–CVM for $A2$ phase using tetrahedron as basic cluster, shown in Figure 3.1, involves five CFs in the orthogonal basis, namely, the point CF (u_0), first neighbour pair CF (u_1), second neighbour pair CF (u_2), triangle CF (u_3) and tetrahedron CF (u_4). The CFs and other essential details used to formulate the configurational Helmholtz energy of mixing (A^{mix}_{A2}) for $A2$ phase are presented in Table 3.1.

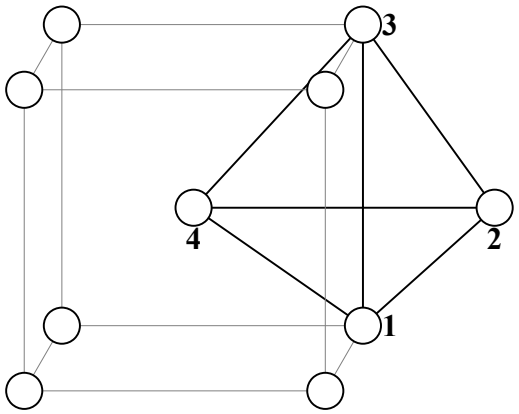

Figure 3.1: The irregular tetrahedron cluster in $A2$ phase.

Table 3.1: The clusters, their CFs, multiplicities (m_i), number of sub-clusters j present in each cluster i (n^k_i) and K-B coefficients (γ_i) for the $A2$ phase using T approximation.

Clusters	CF	m_i	n^4_i	n^3_i	n^2_i	n^1_i	n^0_i	γ_i
Irregular tetrahedron	u_4	6	1	4	2	4	4	1
Isosceles triangle	u_3	12	0	1	1	2	3	-1
II-n pair	u_2	3	0	0	1	0	2	1
I-n pair	u_1	4	0	0	0	1	2	1
Point	u_0	1	0	0	0	0	1	-1

The equilibrium equations for $A2$ phase in the tetrahedron approximation of CE–CVM are obtained using Eq. (2.19). However, since $\xi = 0$, the first equation is not applicable for this disordered phase. The equilibrium equations obtained in this case are as follows:

$$\left[\left[1+u_1\right]^2-4u_0^2\right]\left[\left[1+4u_1+2u_2+u_4\right]^2-16\left[u_0+u_3\right]^2\right]^{3/2}$$
$$\left[\left[1-2u_1+u_2\right]^2-\left[u_0-u_3\right]^2\right]^3-\left[1-u_1\right]^2\left[\left[1+2u_1+u_2\right]^2-\left[3u_0+u_3\right]^2\right]^3 \tag{3.1}$$
$$\left[1-4u_1+2u_2+u_4\right]^3\eta_1=0$$

$$\left[\left[1+u_2\right]^2-4u_0^2\right]\left[\left[1-u_2\right]^2-\left[u_0-u_3\right]^2\right]^4\left[1-4u_1+2u_2+u_4\right]^2$$
$$\left[\left[1+4u_1+2u_2+u_4\right]^2-16\left[u_0+u_3\right]^2\right]-\left[\left[1-2u_1+u_2\right]^2-\left[u_0-u_3\right]^2\right]^2 \tag{3.2}$$
$$\left[1-u_2\right]^2\left[1-2u_2+u_4\right]^4\left[\left[1+2u_1+u_2\right]^2-\left[3u_0+u_3\right]^2\right]^2\eta_2=0$$

$$\left[1+u_0-u_2-u_3\right]^2\left[1+u_0-2u_1+u_2-u_3\right]\left[1-3u_0+2u_1+u_2-u_3\right]$$
$$\left[1-2u_0+2u_3-u_4\right]^2\left[1+4u_0+4u_1+2u_2+4u_3+u_4\right]$$
$$-\left[1-u_0-u_2+u_3\right]^2\left[1-u_0-2u_1+u_2+u_3\right]\left[1+3u_0+2u_1+u_2+u_3\right] \tag{3.3}$$
$$\left[1+2u_0-2u_3-u_4\right]^2\left[1-4u_0+4u_1+2u_2-4u_3+u_4\right]\eta_3=0$$

$$\left[1-2u_2+u_4\right]^4\left[1-4u_1+2u_2+u_4\right]^2\left[\left[1+4u_1+2u_2+u_4\right]^2-16\left[u_0+u_3\right]^2\right]$$
$$-\left[\left[1-u_4\right]^2-4\left[u_0-u_3\right]^2\right]^4\eta_4=0 \tag{3.4}$$

For the case of exclusive second-neighbour pair interactions, $e_2 \neq 0$, while $e_1 = e_3 = e_4 = 0$. An examination of the numerical solutions of the equilibrium equations reveals that u_1 is independent of e_2, and must be equal to its random value of u_0^2 in the limit of infinite temperature ($\eta_2 = 1$). Hence, in general,

$$u_1 = u_0^2 \tag{3.5}$$

Numerical results obtained by solving equilibrium equations conform to the above analytical solution in the entire range of compositions and temperatures.

For an equiatomic alloy ($u_0 = 0$ and accordingly $u_1 = 0$), owing to symmetry, the CFs corresponding to clusters having odd number of sites must vanish, *i.e.*, $u_3 = 0$. For these conditions, the equilibrium equation corresponding to the tetrahedron CF (Eq. (3.4)) can be solved to yield

$$u_4 = u_2^2 \tag{3.6}$$

Further, it is observed that the above solution holds for all values of u_0 and η_2. By substituting from Eqs. (3.5) and (3.6) in the equilibrium equation corresponding to the triangle CF (Eq. (3.3)), one obtains

$$u_3 = u_0 u_2 \tag{3.7}$$

Using these relations, the energy function is as follows

$$\begin{aligned} A_{A2}^{mix} =& 3e_2\left[u_2 - 1\right] + (3/4)\mathrm{R}T\left[\left[1 - 2u_0 + u_2\right]\ln\left[1 - 2u_0 + u_2\right]\right. \\ &+ 2\left[1 - u_2\right]\ln\left[1 - u_2\right] + \left.\left[1 + 2u_0 + u_2\right]\ln\left[1 + 2u_0 + u_2\right]\right] \\ &- (5/2)\mathrm{R}T\left[\left[1 - u_0\right]\ln\left[1 - u_0\right] + \left[1 + u_0\right]\ln\left[1 + u_0\right]\right] - \mathrm{R}T\ln\left[2\right] \end{aligned} \tag{3.8}$$

Thus, the equilibrium equation corresponding to the second neighbour pair CF becomes,

$$\left(u_2 + 1\right)^2 - \left(u_2 - 1\right)^2 \eta_2 - 4u_0^2 = 0 \tag{3.9}$$

This is a quadratic equation in u_2 and can be solved in terms of u_0 and η_2. The solution that reproduces the correct random value for the case of $\eta_2 = 1$ is as follows.

$$u_2 = \frac{1 + \eta_2 - 2\sqrt{\eta_2 - u_0^2\left(\eta_2 - 1\right)}}{\eta_2 - 1} \tag{3.10}$$

It is interesting to note that this result is identical to that for the case of quasi-chemical model in pair approximation (Guggenheim, 1952). The solutions obtained for the CFs in Eqs. (3.5)–(3.7) & (3.10) analytically satisfy the equilibrium equations in Eqs. (3.1)–(3.4) for the case of exclusive second neighbour pair interactions.

The Helmholtz energy becomes a function only of u_0 and η_2 after substitution of the above analytical solutions of CFs for exclusive second neighbour pair interactions. The consolute point of miscibility gap in a phase separating system can be determined by simultaneously requiring the second and third derivatives of the Helmholtz energy with respect to composition to vanish. The consolute point is thus found to be

$$u_0 = 0 \;\text{ and }\; \eta_{2c}^{\mathrm{PS}} = \frac{9}{4} \;\text{ or }\; T_c^{\mathrm{PS}} = -\frac{4e_2}{\mathrm{R}\ln\left(9/4\right)} \tag{3.11}$$

The miscibility gap boundary is thus given by

$$\frac{T}{T_c^{\mathrm{PS}}} = \frac{\ln\left(9/4\right)}{\ln\left[\frac{4u_0^2}{\left(1-u_0^2\right)^{1/3}\left[\left(1-u_0\right)^{2/3} - \left(1+u_0\right)^{2/3}\right]^2}\right]} \tag{3.12}$$

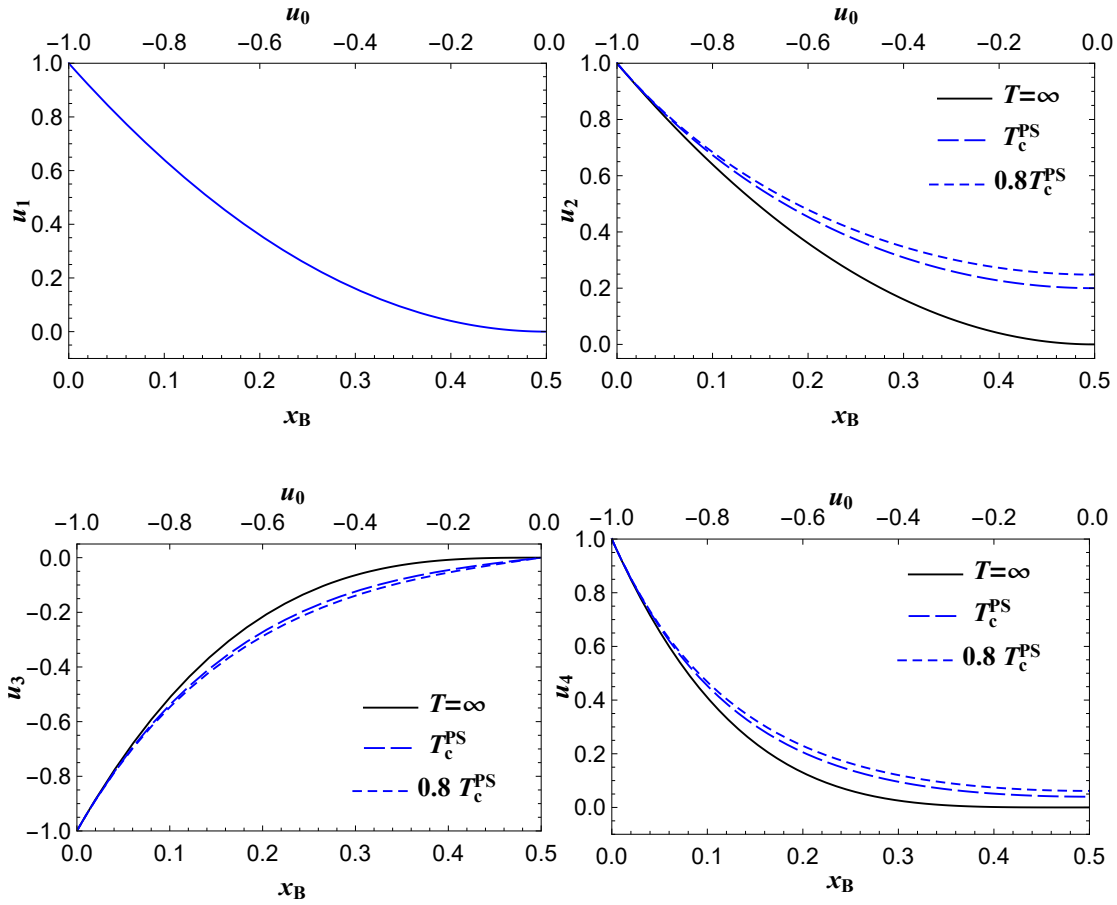

Figure 3.2: Variation of CFs for first neighbour pair (u_1), second neighbour pair (u_2), triangle (u_3) and tetrahedron (u_4) clusters with respect to composition at different temperatures for phase separating system. The miscibility gap boundaries are located at $x_{\mathrm{B}} = 0.104$ and 0.896 for $T = 0.8\ T_{\mathrm{c}}^{\mathrm{PS}}$.

Analytical solution for the spinodal boundary is given by

$$\eta_2 = \frac{(9/4) - u_0^2}{1 - u_0^2} \quad \text{or} \quad u_0 = \pm\sqrt{\frac{\eta_2 - (9/4)}{\eta_2 - 1}} \quad \text{or} \quad \frac{T}{T_{\mathrm{c}}^{\mathrm{PS}}} = \frac{\ln(9/4)}{\ln\left[\frac{(9/4)-u_0^2}{1-u_0^2}\right]} \tag{3.13}$$

The variation of all CFs with respect to composition at various temperatures is given in Figure 3.2 for phase separating systems. The miscibility gap and the spinodal boundaries calculated using Eqs. (3.12) and (3.13) are depicted in Figure 3.3.

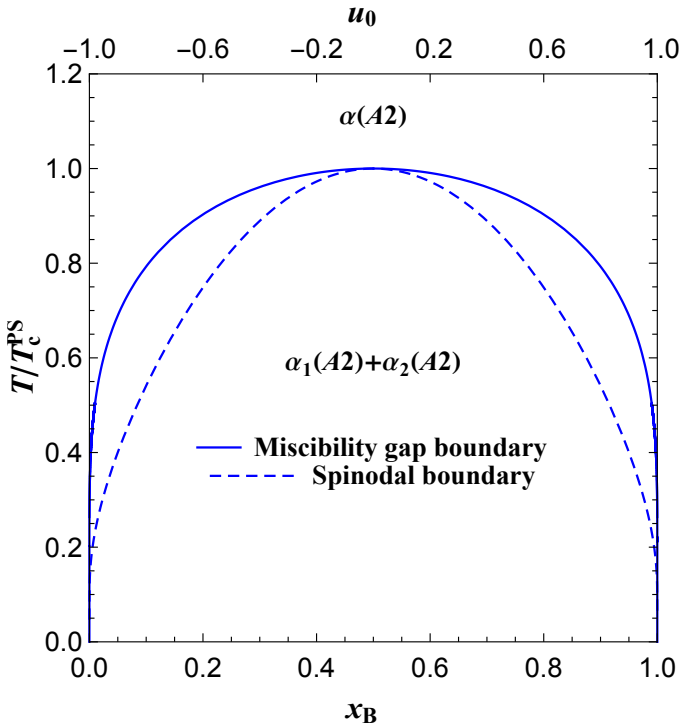

Figure 3.3: Miscibility gap boundary and spinodal boundary calculated using the analytical solutions.

3.3 Analytical solutions for CFs in $B32$ phase

The irregular tetrahedron cluster used to obtain Helmholtz energy expression for $B32$ phase can be found in Figure A.1. The details of the subclusters, the corresponding CFs, their multiplicities and the K-B coefficients used in the present formulation is provided in Table A.1.

The point CFs $u_{0.1}$ and $u_{0.2}$ in $B32$ phase corresponding to the sublattice sites α and β respectively are related to u_0 and ξ, through

$$u_0 = \frac{u_{0.1} + u_{0.2}}{2} \quad \text{and} \quad \xi = \frac{u_{0.2} - u_{0.1}}{2} \tag{3.14}$$

The first neighbour pair CF u_1 in the $A2$ phase splits into three pair CFs in $B32$ phase namely, $u_{1.1}$, $u_{1.2}$ and $u_{1.3}$ corresponding to site occupancies on $\alpha\alpha$, $\alpha\beta$ and $\beta\beta$ sublattice sites respectively. In analogy with Eq. (3.5) for the $A2$ phase, the first neighbour pair CFs in $B32$ phase satisfy the following relations

$$u_{1.1} = u_{0.1}^2,\ u_{1.2} = u_{0.1}u_{0.2} \ \text{ and } \ u_{1.3} = u_{0.2}^2 \tag{3.15}$$

which is confirmed from numerical results. In an analogous manner, the triangle and

tetrahedron CFs in $B32$ phase can be seen to satisfy the following relations

$$u_{3.1} = u_{0.1}u_{2.1},\ u_{3.2} = u_{0.2}u_{2.1} \text{ and } u_{4.1} = u_{2.1}^2 \tag{3.16}$$

By substituting from Eqs. (3.15) and (3.16), the simplified expression for Helmholtz energy is given by

$$\begin{aligned} A_{B32}^{mix} =& 3e_2\left(u_{2.1}-1\right) + (3/4)\mathrm{R}T\left[\left(1+2u_0+u_{2.1}\right)\ln\left(1+2u_0+u_{2.1}\right)\right. \\ &+\left(1-2u_0+u_{2.1}\right)\ln\left(1-2u_0+u_{2.1}\right)+\left(1+2\xi-u_{2.1}\right)\ln\left(1+2\xi-u_{2.1}\right) \\ &\left.+\left(1-2\xi-u_{2.1}\right)\ln\left(1-2\xi-u_{2.1}\right)\right] - (5/4)\mathrm{R}T\left[\left(1+u_0+\xi\right)\ln\left(1+u_0+\xi\right)\right. \\ &+\left(1-u_0+\xi\right)\ln\left(1-u_0+\xi\right)+\left(1+u_0-\xi\right)\ln\left(1+u_0-\xi\right) \\ &\left.+\left(1-u_0-\xi\right)\ln\left(1-u_0-\xi\right)\right] - \mathrm{R}T\ln(2) \end{aligned} \tag{3.17}$$

The equilibrium conditions can be obtained by minimizing the Helmholtz energy with respect to ξ and $u_{2.1}$ respectively and are given below.

$$\left[\left(1-\xi\right)^2-u_0^2\right]^5\left(1-u_{2.1}+2\xi\right)^6-\left[\left(1+\xi\right)^2-u_0^2\right]^5\left(1-u_{2.1}-2\xi\right)^6=0 \tag{3.18}$$

$$\left(1-2u_0+u_{2.1}\right)\left(1+2u_0+u_{2.1}\right)+\eta_2\left(1-2\xi-u_{2.1}\right)\left(1+2\xi-u_{2.1}\right)=0 \tag{3.19}$$

The equilibrium condition in Eq. (3.19) is a quadratic in $u_{2.1}$, which can be solved for $u_{2.1}$ in terms of η_2, u_0 and ξ. The solution that reproduces the correct value for $\eta_2 \to 1$ corresponding to random occupation of the sites in each of the sublattices is given by

$$u_2 = \frac{1+\eta_2-2\sqrt{\eta_2-\left(u_0^2-\eta_2\xi^2\right)\left(\eta_2-1\right)}}{\eta_2-1} \tag{3.20}$$

It may be noted that the complete set of solutions given in Eqs. (3.15), (3.16) and (3.20) analytically satisfy the equilibrium equations.

An explicit solution for ξ in terms of u_0 and η_2 is not possible. However, it is possible to express η_2 as a function of u_0 and ξ as follows. The equilibrium equation for ξ, *i.e.*, Eq. (3.18), can be rearranged to give

$$\frac{1-u_{2.1}+2\xi}{1-u_{2.1}-2\xi} = \left[\frac{\left(\xi+1\right)^2-u_0^2}{\left(\xi-1\right)^2-u_0^2}\right]^{5/6} = Y, \text{ say} \tag{3.21}$$

The above equation can be solved for $u_{2.1}$ in terms of Y to yield

$$u_{2.1} = 1-2\xi\left(\frac{Y+1}{Y-1}\right) \tag{3.22}$$

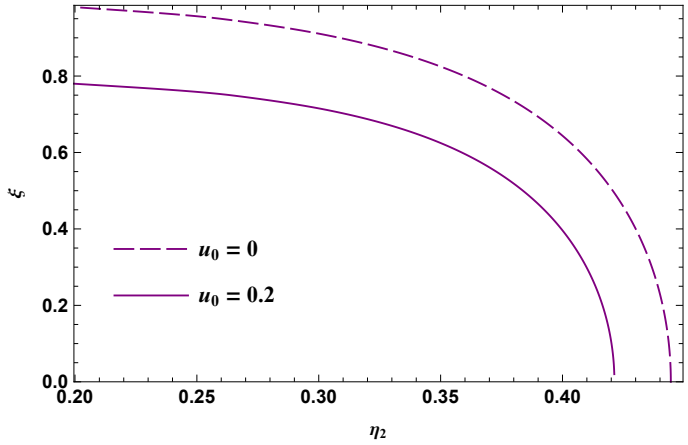

Figure 3.4: Variation of order parameter with η_2 for $B32$ phase at $u_0 = 0$ and $u_0 = 0.2$.

Substituting this relation in Eq. (3.19) and solving for η_2 gives

$$\eta_2 = \frac{\left[(Y-1) - \xi\,(Y+1)\right]^2 - u_0^2\,(Y-1)^2}{4\xi^2 Y} \tag{3.23}$$

Here Y is a function of u_0 and ξ. The equilibrium value of ξ at chosen temperature and composition can be found by numerically solving Eq. (3.23). However, the values of η_2 for which the selected values of u_0 and ξ remain in equilibrium can be found directly.

For ordering systems, the solutions for the second neighbour pair correlation function for the $A2$ and $B32$ phases (given respectively by Eqs. (3.10) and (3.20)) at T= 0 K (*i.e.*, η_2=0) become identical and reduce to the following.

$$u_{2.1} = -1 + 2|u_0| = u_2 \tag{3.24}$$

The equilibrium value of ξ at 0 K can be found by substituting from Eq. (3.24) in the equilibrium condition for ξ, *i.e.*, Eq. (3.18). After simplification, this equation becomes a quintic in ξ. One of the solutions of this equation is $\xi = 0$, which corresponds to the unstable disordered state of the system. On factoring out ξ, the physically relevant solution of the resultant quartic is as under.

$$\xi^{0\mathrm{K}} = (1 + |u_0|)\sqrt{\frac{-5|u_0| + 2\sqrt{1+4u_0^2}}{2+3|u_0|}} \tag{3.25}$$

The variation of ξ with η_2 at two different compositions, viz., u_0 = 0 and u_0 = 0.2 is shown in Figure 3.4. This indicates that $A2$–$B32$ transformation is of second order and the critical point can be calculated by simultaneously solving the following equations

$$\frac{\partial A_{B32}^{mix}}{\partial \xi} = 0, \frac{\partial^2 A_{B32}^{mix}}{\partial \xi^2} = 0 \text{ and } \frac{\partial^3 A_{B32}^{mix}}{\partial \xi^3} = 0 \tag{3.26}$$

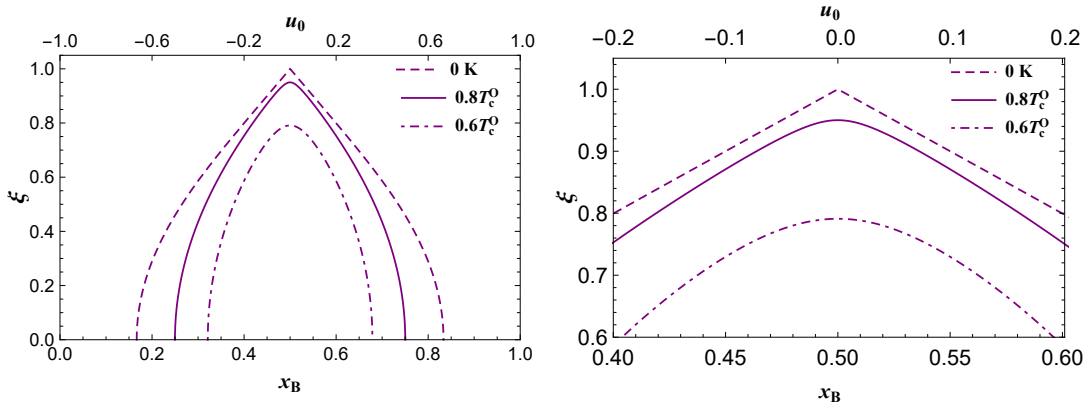

Figure 3.5: Variation of order parameter with composition at different values of T/T_c^O.

It may be noted that the first one of the above equations is the equilibrium condition given in Eq. (3.18). The critical point thus calculated is given by

$$u_0^c = 0 \text{ and } \eta_{2c}^O = \frac{4}{9} \text{ or } T_c^O = -\frac{4e_2}{R \ln(4/9)} \tag{3.27}$$

The locus of $A2$–$B32$ phase boundary is calculated by solving the first equation in Eq. (3.26) along with the equilibrium condition in Eq. (3.18) and is given below.

$$\eta_2 = \frac{(4/9) - u_0^2}{1 - u_0^2} \text{ or } u_0 = \pm\sqrt{\frac{(4/9) - \eta_2}{1 - \eta_2}} \text{ or } \frac{T}{T_c^O} = \ln(4/9)/\ln\left[\frac{(4/9) - u_0^2}{1 - u_0^2}\right] \tag{3.28}$$

Using the above equation, the limiting values of composition corresponding to $\eta_2 = 0$ for $A2$–$B32$ phase boundary can be obtained as $u_0 = \pm 2/3$. These points are represented with vertical arrow marks in the relevant Figures of the present Chapter. Further, for $T_c^O/2$, the phase boundary composition can be obtained as $\pm\sqrt{4/13}$. The variation of ξ with composition at various temperatures is evaluated by using the corresponding equilibrium equation and Eq. (3.25) and is shown in Figure 3.5.

Subsequent to the numerical (for $T \neq 0$ K) or analytical (at $T = 0$ K) evaluation of the equilibrium value of ξ, the CFs can be found using analytical results given above (Eqs. (3.15), (3.16) and (3.20)). The variation of CFs for the $A2$ and $B32$ phases as a function of composition at various temperatures is shown in Figure 3.6.

The $A2$–$B32$ phase boundary calculated using Eq. (3.28) is depicted in Figure 3.7. It may be noted that this boundary is in fact a spinodal ordering boundary and not a true phase boundary, since the transformation $A2 \rightarrow B32$ is of second order.

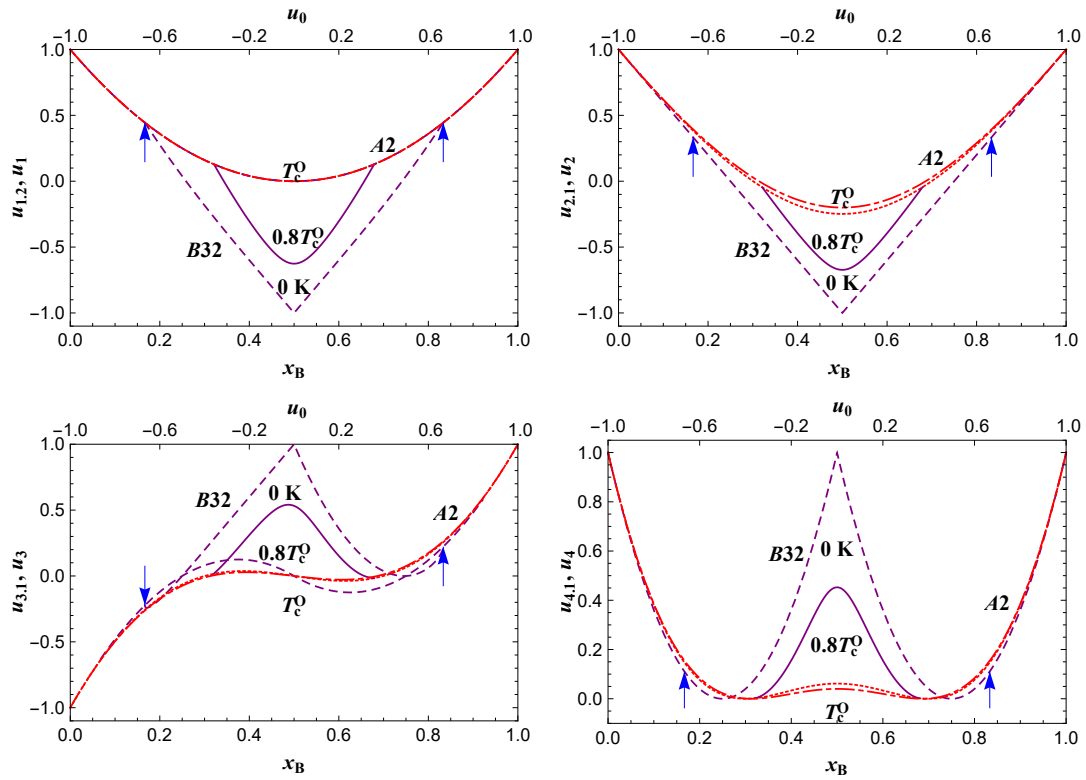

Figure 3.6: Variation of CFs for $A2$ and $B32$ phases with composition at 0 K, $0.8T_c^O$ and T_c^O. The phase boundaries at 0 K are located at $x_B = (1/6, 5/6)$ and are represented by vertical arrows.

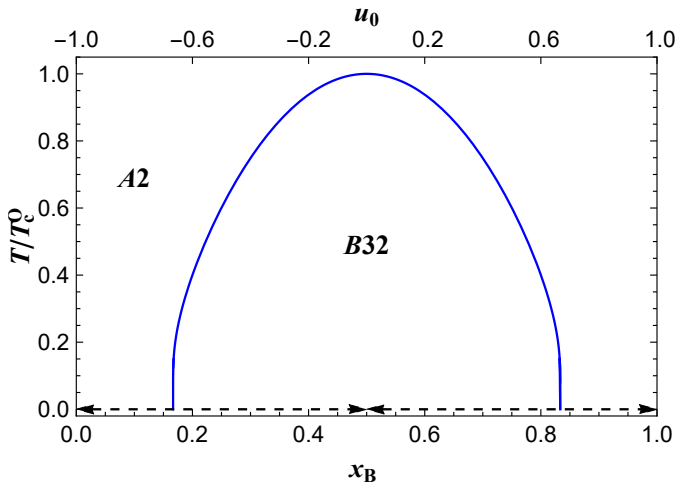

Figure 3.7: The $A2$–$B32$ phase boundary calculated using the analytical solution. The dashed lines with arrowheads at $T = 0$ K indicate degenerate states as explained in the text in Section 3.5.

3.4 Analytical solutions for CFs in $A1$ and $L1_1$ phases

The details of the CFs under TO approximation for $A1$ phase can be found elsewhere (Sarma *et al.*, 2012). The solutions for all CFs of $A1$ phase can be found in terms of u_0 and u_2 for the case of exclusive second neighbour pair interactions, guided by the numerical results and symmetry requirements. They satisfy the following relations.

$$\begin{aligned} &u_1 = u_0^2; \quad u_3 = u_0^3; \quad u_4 = u_0 u_2; \quad u_5 = u_0^4 \\ &u_6 = u_0^2 u_2; \quad u_7 = u_2^2; \quad u_8 = u_0 u_2^2; \quad u_9 = u_2^3 \end{aligned} \tag{3.29}$$

The above relations can be substituted in the equilibrium equation corresponding to u_2 and the simplified equilibrium equation can be solved for u_2 to yield

$$u_2 = \frac{1 + \eta_2 - 2\sqrt{\eta_2 - u_0^2\,(\eta_2 - 1)}}{\eta_2 - 1} \tag{3.30}$$

which is identical to the solution obtained for the case of second neighbour pair CF for $A2$ phase given in Eq. (3.10).

The tetrahedron and octahedron clusters considered in the $L1_1$ phase can be found in Figure A.6. The two point CFs are related to u_0 and ξ as given in Eq. (3.14). The details of the clusters, the corresponding ordered cluster, their designations $(i.j)$, multiplicities and the K-B coefficients can be found in Table A.6.

The Helmholtz energy is obtained using the above details as discussed in Section 2.2. The CFs of $L1_1$ phase for exclusive second neighbour pair interactions are related to $u_{0.1}, u_{0.2}$ and $u_{2.1}$ as under

$$\begin{aligned} &u_{1.1} = u_{0.1}^2; && u_{1.2} = u_{0.1}u_{0.2}; && u_{1.3} = u_{0.2}^2 \\ &u_{3.1} = u_{0.1}^3; && u_{3.2} = u_{0.1}^2 u_{0.2}; && u_{3.3} = u_{0.1}u_{0.2}^2 \\ &u_{3.4} = u_{0.2}^3; && u_{4.1} = u_{0.1}u_{2.1}; && u_{4.2} = u_{0.2}u_{2.1} \\ &u_{5.1} = u_{0.1}^3 u_{0.2}; && u_{5.2} = u_{0.1}u_{0.2}^3; && u_{6.1} = u_{0.1}^2 u_{2.1} \\ &u_{6.2} = u_{0.1}u_{0.2}u_{2.1}; && u_{6.3} = u_{0.2}^2 u_{2.1}; && u_{7.1} = u_{2.1}^2 \\ &u_{8.1} = u_{0.1}u_{2.1}^2; && u_{8.2} = u_{0.2}u_{2.1}^2; && u_{9.1} = u_{2.1}^3 \end{aligned} \tag{3.31}$$

Substitution of the above relations into Helmholtz energy expression reduces it to the one identical to that of $B32$ phase given in Eq. (3.17). The simplified equilibrium

equation corresponding to the CF $u_{2.1}$ can be solved to obtain the following solution that returns the correct numerical values.

$$u_{2.1} = \frac{1 + \eta_2 - 2\sqrt{\eta_2 - (u_0^2 - \eta_2\xi^2)\,(\eta_2 - 1)}}{\eta_2 - 1} \tag{3.32}$$

Therefore, the results given in the above Sections 3.2, 3.3 and the subsequent Sections are equally valid for the present case as well.

3.5 Helmholtz energy

For the ordering system $A2$–$B32$, the configurational energy of mixing ($U^{mix}/\mathrm{R}T_c^{\mathrm{O}}$) and entropy of mixing (S^{mix}/R) are calculated at 0 K and $T_c^{\mathrm{O}}/2$ and are shown in Figure 3.8. In addition, the configurational Helmholtz energy is also plotted at the above temperatures and is shown in Figure 3.9.

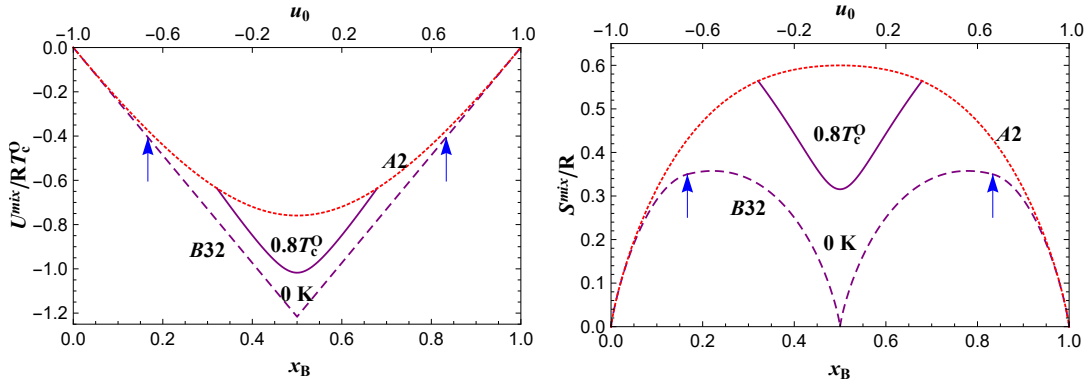

Figure 3.8: Variation of configurational energy of mixing ($U^{mix}/\mathrm{R}T_c^{\mathrm{O}}$) and entropy of mixing (S^{mix}/R) with composition for $A2$ and $B32$ phases at 0 K and $T_c^{\mathrm{O}}/2$.

Note that the value of the Helmholtz function at a particular composition becomes equal to that of the configurational energy of mixing at the same composition at $T = 0\,\mathrm{K}$ since the entropy term vanishes at this temperature. Further, the configurational energies of mixing for the $A2$ and $B32$ phases reduce to the same value at $T = 0$ K.

$$A_{A2}^{mix} = A_{B32}^{mix} = 3e_2\,(u_2 - 1) = -6e_2\,(1 - |u_0|) \tag{3.33}$$

It can be observed that the Helmholtz energy expression is independent of ξ and a linear function of composition (Figure 3.9). For $T \neq 0$ K, the microscopic state of the system, governed by u_2 for $A2$ phase and $u_{2.1}$ for $B32$ phase, are different for the selected u_0 value inside $A2$–$B32$ boundary. For that T and composition, the

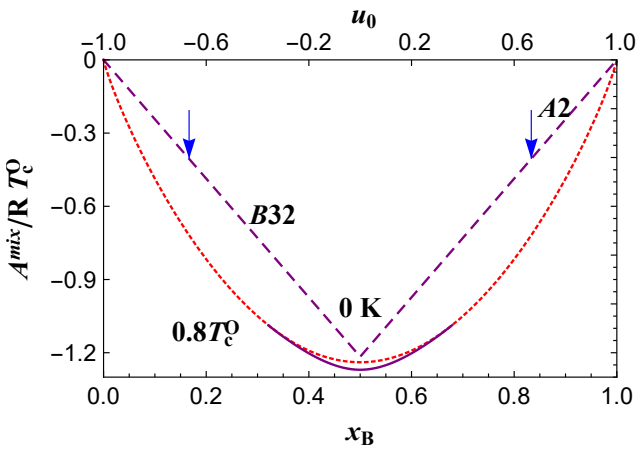

Figure 3.9: Variation of Helmholtz energy with composition for $A2$ and $B32$ phases at 0 K and 0.8 T_c^O.

Helmholtz energy of mixing for $B32$ phase is lower than that of mechanical mixture of any other states in the entire composition range. However at T = 0 K, both the ordered and disordered phases have reduced to the same microscopic state and have same Helmholtz energy. This value is also equal to the weighted sum of the fraction of the pure A (or B) phase and fraction of $B32$ phase obtained by lever rule multiplied with the respective Helmholtz energies. This also shows that the system can posses lower Helmholtz energy with multiple microscopic states. This clearly indicates a state of degeneracy and apparent violation of the third law of thermodynamics. Abriata and Laughlin (2004) have discussed in detail about the significance of the third law of thermodynamics in the determination of phase diagrams by considering a few real systems. Laughlin and Soffa (2018) have considered Bragg-Williams model for $B2$ phase and shown that for exclusive first pair interactions, the variation of Helmholtz energy at 0 K is similar to that of $A2$–$B32$ phases shown in Figure 3.9 and the system shows a state of degeneracy. The possible topologies of the phase diagrams for mixed pair interactions have also been discussed. They have shown that this arises owing to exclusive single pair interactions independently of the accuracy of the model. This state is represented by a dashed arrow in Figure 3.7.

3.6 Heat capacity

The configurational heat capacity of mixing of the disordered phase is given by

$$\begin{aligned} C_v^{A2} &= \frac{dU_{A2}^{mix}}{dT} = \frac{\partial U_{A2}^{mix}}{\partial u_2}\frac{\partial u_2}{\partial \eta_2}\frac{d\eta_2}{dT} \\ &= \frac{3\mathrm{R}\left(1-u_0^2\right)^2 \eta_2 \ln \eta_2}{2\sqrt{u_0^2+\eta_2\left(1-u_0^2\right)}\left(1+\sqrt{u_0^2+\eta_2\left(1-u_0^2\right)}\right)^2} \end{aligned} \tag{3.34}$$

Similarly, the configurational heat capacity of mixing of the ordered phase is given by

$$C_v^{B32} = \frac{dU_{B32}^{mix}}{dT} = \left(\frac{\partial U_{B32}^{mix}}{\partial u_{2.1}}\frac{\partial u_{2.1}}{\partial \eta_2} + \frac{\partial U_{B32}^{mix}}{\partial \xi}\frac{\partial \xi}{\partial \eta_2}\right)\frac{d\eta_2}{dT} \tag{3.35}$$

The required derivatives can be evaluated using Eqs. (3.20) and (3.23). The difference in the heat capacity of the two phases at the phase boundary ($\xi = 0$) is given by

$$\Delta C_v = C_v^{B32} - C_v^{A2} = \frac{\partial U_{B32}^{mix}}{\partial \xi}\frac{\partial \xi}{\partial \eta_2}\frac{d\eta_2}{dT} \tag{3.36}$$

Using the analytical solution of the boundary provided in Eq. (3.28), the difference in the heat capacity at the boundary becomes

$$\Delta C_v = \frac{27\mathrm{R}\left(1-u_0^2\right)\left[\left(4-9u_0^2\right)\ln\left(\frac{(4/9)-u_0^2}{1-u_0^2}\right)\right]^2}{40\left(4+27u_0^2\right)} \tag{3.37}$$

The variation of heat capacity with composition at $T_c^{\mathrm{O}}/2$ is shown in Figure 3.10 (a). The difference in heat capacity at equiatomic composition using Eq. (3.37) is identical to that found by Guggenheim (1952) using quasi-chemical theory in pair approximation with coordination number, z = 6 in his eq. 7.18.3.

In the heat capacity plot shown in Figure 3.10 (a), there is an anomalous peak in the heat capacity of the ordered $B32$ phase near the stoichiometric composition, the variation of which with changing temperature is depicted in Figure 3.10 (b). It may be noted that the peak diminishes gradually, with a decrease in its height as well as breadth as the temperature decreases and eventually disappears at 0 K. Further, it may be pointed out that the compositions corresponding to the minima in the C_v curve spread out on either side of the equiatomic composition with increasing temperature and become equal to the composition of the phase boundary at around $T = 0.84\ T_c^{\mathrm{O}}$.

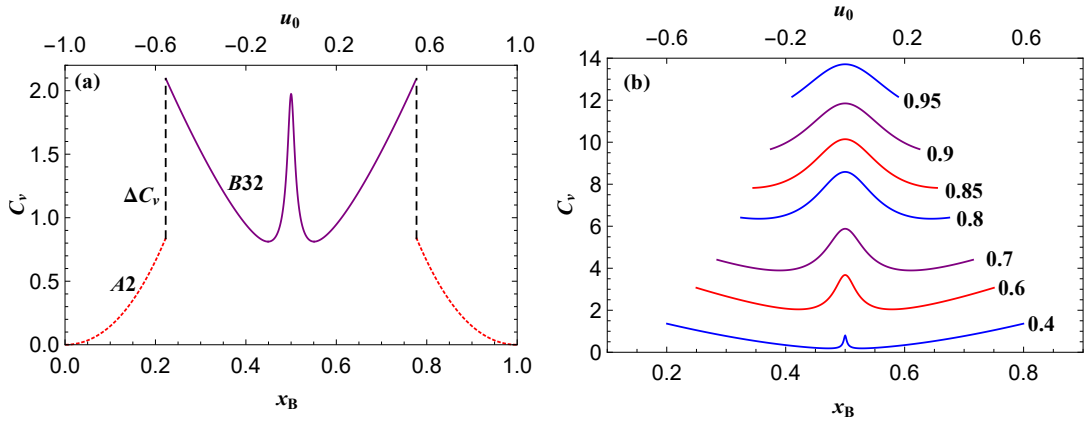

Figure 3.10: (a) Variation of heat capacity with composition for $A2$ and $B32$ phases at $T_c^O/2$. (b) Variation of heat capacity with composition for the $B32$ phase at different T/T_c^O temperatures. The minima in C_v are located at x_B = (0.4715, 0.5285), (0.4215, 0.5785) and (0.3550, 0.6450) at T= $0.4T_c^O$, $0.6T_c^O$ and $0.8T_c^O$ respectively.

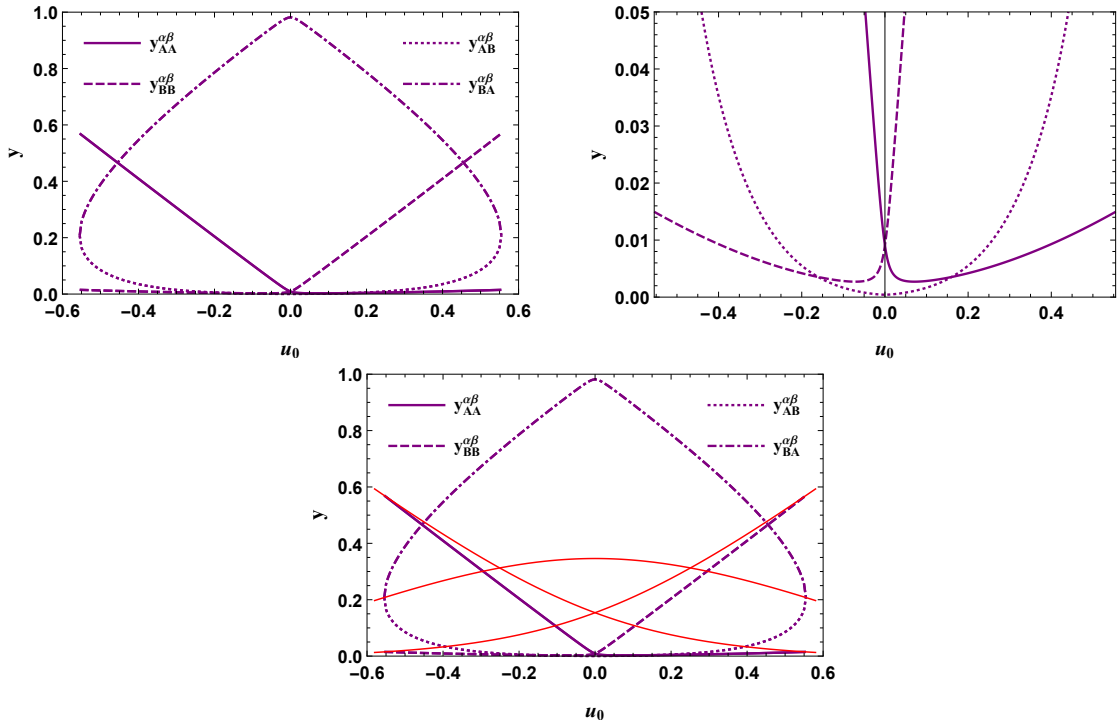

Figure 3.11: The variation of CVs with point CF (u_0) at $0.5T_c^O$. The thin red lines indicate the corresponding CVs in the disordered phase.

The variation of order parameter (ξ) with composition is shown in Figure 3.5. From the figure it can be observed that the departure of order parameter from its maximum value has a minimum for composition away from the stoichiometric composition (u_0 = 0). Using the order parameter calculated numerically and the analytical solutions obtained for the CF, the value of the CVs are calculated with composition and is shown in Figure 3.11. From the figure, it can be observed that the

CVs, $y_{\mathrm{AA}}^{\alpha\beta}$ and $y_{\mathrm{BB}}^{\alpha\beta}$, have a minimum away from the stoichiometric composition like order parameter. It was mentioned that this behaviour is due to variation of ordering on the sublattices. This anomalous behaviour in heat capacity has also been reported earlier and explained by different authors (Kusoffsky and Sundman, 1998; Schön and Inden, 1998; Sluiter and Kawazoe, 1999).

3.7 Thermodynamic stability function (ψ)

The thermodynamic stability function ψ (Lupis, 1983) which is also known as the thermodynamic factor ϕ (Balogh and Schmitz, 2014) in diffusion literature is defined as

$$\psi = x_{\mathrm{A}} x_{\mathrm{B}} \frac{d^2 G^{mix}/\mathrm{R}T}{dx_{\mathrm{B}}^2} = \left(1 - u_0^2\right) \frac{d^2 G^{mix}/\mathrm{R}T}{du_0^2} \tag{3.38}$$

The Gibbs energy will be approximated by the Helmholtz energy, which is valid for condensed phases. Using Eqs. (3.8) and (3.10), the thermodynamic stability function for $A2$ phase can be directly evaluated. However, the thermodynamic stability function for $B32$ phase involves variation of ξ with respect to x_{B} as given below.

$$\psi_{B32} = x_{\mathrm{A}} x_{\mathrm{B}} \left[\left(\frac{\partial^2 G_{B32}^{mix}}{\partial x_{\mathrm{B}}^2} \right)_{\xi} + \left(\frac{\partial}{\partial \xi} \left(\frac{\partial G_{B32}^{mix}}{\partial x_{\mathrm{B}}} \right)_{\xi} \right)_{x_{\mathrm{B}}} \frac{d\xi}{dx_{\mathrm{B}}} \right] \tag{3.39}$$

For evaluating the differential $(d\xi/dx_{\mathrm{B}})$ in Eq. (3.39), consider the total differential of the order parameter equilibrium equation with respect to x_{B}, which can be written as

$$\frac{d}{dx_{\mathrm{B}}} \left(\frac{\partial G_{B32}^{mix}}{\partial \xi} \right)_{x_{\mathrm{B}}} = \left(\frac{\partial}{\partial x_{\mathrm{B}}} \left(\frac{\partial G_{B32}^{mix}}{\partial \xi} \right)_{x_{\mathrm{B}}} \right)_{\xi} + \left(\frac{\partial^2 G_{B32}^{mix}}{\partial \xi^2} \right)_{x_{\mathrm{B}}} \frac{d\xi}{dx_{\mathrm{B}}} = 0 \tag{3.40}$$

Accordingly,

$$\frac{d\xi}{dx_{\mathrm{B}}} = -\left(\frac{\partial}{\partial x_{\mathrm{B}}} \left(\frac{\partial G_{B32}^{mix}}{\partial \xi} \right)_{x_{\mathrm{B}}} \right)_{\xi} \Bigg/ \left(\frac{\partial^2 G_{B32}^{mix}}{\partial \xi^2} \right)_{x_{\mathrm{B}}} \tag{3.41}$$

Substitution for $(d\xi/dx_{\mathrm{B}})$ from Eq. (3.41) in Eq. (3.39) yields an expression for ψ which can be evaluated at any composition and temperature after determining ξ from equilibrium equations. However, this equation breaks down for ξ =0 at the $A2$–$B32$ phase boundary. To evaluate the difference in the stability function $\Delta\psi = \psi_{B32} - \psi_{A2}$, at the $A2$–$B32$ phase boundary where the compositions are identical for both the phases and $\xi = 0$ in the $B32$ phase, we note that

$$\left(\frac{\partial^2 G_{B32}^{mix}}{\partial x_{\mathrm{B}}^2} \right)_{\xi} = \frac{\partial^2 G_{A2}^{mix}}{\partial x_{\mathrm{B}}^2} \tag{3.42}$$

Thus, at the phase boundary

$$\begin{aligned}\Delta\psi &= -x_{\mathrm{A}}x_{\mathrm{B}}\left(\frac{\partial}{\partial\xi}\left(\frac{\partial G^{mix}_{B32}}{\partial x_{\mathrm{B}}}\right)_{\xi}\right)_{x_{\mathrm{B}}}\frac{d\xi}{dx_{\mathrm{B}}} \\ &= -\frac{x_{\mathrm{A}}x_{\mathrm{B}}}{2\xi}\left(\frac{\partial}{\partial\xi}\left(\frac{\partial G^{mix}_{B32}}{\partial x_{\mathrm{B}}}\right)_{\xi}\right)_{x_{\mathrm{B}}}\frac{d\xi^2}{dx_{\mathrm{B}}}\end{aligned} \tag{3.43}$$

At the phase boundary, the differential terms in the numerator as well as the denominator in Eq. (3.41) vanish, making their ratio indeterminate. It can be evaluated by considering

$$\frac{d\xi^2}{dx_{\mathrm{B}}} = 2\xi\frac{d\xi}{dx_{\mathrm{B}}} = -2\xi\left(\frac{\partial}{\partial x_{\mathrm{B}}}\left(\frac{\partial G^{mix}_{B32}}{\partial\xi}\right)_{x_{\mathrm{B}}}\right)_{\xi}\Bigg/\left(\frac{\partial^2 G^{mix}_{B32}}{\partial\xi^2}\right)_{x_{\mathrm{B}}} \tag{3.44}$$

By evaluating the derivatives present on the RHS, as explained in detail in the Appendix B, we have

$$\Delta\psi = \frac{135u_0^2}{8+54u_0^2} = \frac{60-135\eta_2}{32-62\eta_2} \tag{3.45}$$

The analytical value for the difference in stability function provided in Eq. (3.45) agrees well with the numerical values. The variation of the stability function with respect to composition at $T_{\mathrm{c}}^{\mathrm{O}}/2$ is shown in Figure 3.12.

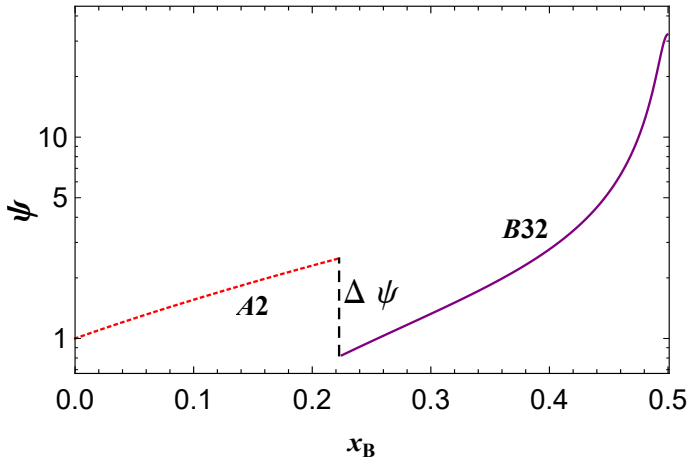

Figure 3.12: Variation of stability function with respect to composition at $T_{\mathrm{c}}^{\mathrm{O}}/2$.

3.8 Applications

The solutions of the CFs (given in Eqs. (3.10), (3.7) and (3.6)) at a fixed composition are continuous functions of η_2, which remain finite for all temperatures. Such rational function (RF)forms can be used as an alternative to those suggested by Kaptay (2014; 2017) for the parameters in R-K polynomials. These RF forms are expected to be well behaved unlike the case of, say, linear model (Kaptay, 2014) given by $L_j = a_j + b_j T$.

Further, the analytical solutions obtained for the CFs reduce to simple RF of η_2 for a selected composition. So, the coefficients of polynomials used to approximate the CFs can be written as RFs of η. The derivation of these polynomial functions and the method to determine the parameters of the RFs is discussed in the next Chapter.